J Porous Mater (2016) 23:1255–1260
DOI 10.1007/s10934-016-0184-1

Effect of phosphorus on acidity and catalytic performance of Al-MCM-41 for the selective conversion of ethyl mercaptan to ethylene and H_2S

Xiong-fei Zhang[1] · Fei Liu[1] · Xiaoxia Yang[1]

Published online: 6 May 2016

Abstract A series of phosphorus modified Al-MCM-41 molecular sieves with various P/Al ratios were prepared via impregnating method and tested in the selective transformation of ethyl mercaptan into ethylene and hydrogen sulfide. The resulting samples were characterized by a combination of X-ray diffraction, N_2 adsorption, ICP-OES, NH_3 -TPD, ^{27}Al and ^{31}P MAS NMR spectroscopy. The experimental findings demonstrated that P modification can effectively increase the concentration as well as the strength of weak acid sites. Intermediate acid sites were gradually decreased with phosphorus addition, and the product distribution was found to vary with the acidity of the zeolites. Phosphorus content has strong influence on catalytic stability and ethylene selectivity. Upon P treatment, the amount of coke drastically decreased and the catalyst lifetime prolonged. The notable results could be useful for developing a viable process for removing ethyl mercaptan from natural gas.

Keywords Ethyl mercaptan · P modification · Al-MCM-41 zeolite · Gas desulphurization

1 Introduction

Sulfur-containing compounds are the major impurities in natural gas, which are very harmful to the environment [1]. With the stringent specifications, the sulfur contents should be reduced to below 5 ppmv and even lower in the near future [2–4]. The traditional Claus deacidification process can efficiently eliminated hydrogen sulfide from the natural gas. However, the gas still contains more than 30 ppmv total sulfur and mainly present in the form of C1–C3 mercaptans, which have strong pungent and undesirable odors [1, 2]. It needs to remove these compounds prior to further processing or transporting to prevent pollution and to protect equipment [5, 6]. In consequence, the deep reduction of the mercaptans from natural gas has attracted more and more attention.

At present, the main processes for the elimination of mercaptans on industrial scale are alkaline treatment, hydro-desulfurization and reaction with olefins [7]. In most of these works, a large amount of reagents must be added and face the problems of waste generation and partial conversion. An alternative way to eliminate mercaptans is selectively transforming mercaptans into hydrocarbons and hydrogen sulfide in the presence of catalysts. The produced hydrogen sulfide can be removed through subsequent deacidification process.

Various solid acid catalysts have been investigated for this reaction, such as alkaline earth, transition metals and zeolites. Among them, zeolites were thought to be superior to others due to their particular porosity and acidity. Cammarano et al. [1] have applied ZSM-5 with various Si/Al ratios, Ferrierite, Y, SAPO-34 to the decomposition of ethyl mercaptans. Their experimental results confirm that the conversion of ethyl mercaptan into ethylene and hydrogen sulfide can be successfully achieved in the presence of zeolites. However, the formation of significant amounts of coke, diethylsulphide and aromatics still accelerated the deactivation of the catalysts, makes this process unviable for industrial applications. There is a need to search for the zeolites that exhibit better catalytic performance, especially for prolonged lifetime.

✉ Xiaoxia Yang
xxy@tju.edu.cn

[1] School of Chemical Engineering and Technology, Tianjin University, Tianjin 300072, People's Republic of China

Recent studies show that MCM-41 has excellent anti-coking ability and a modified MCM-41 structure zeolite with moderate acidity and pore structure may be promising for this reaction [8]. Pure Si-MCM-41 almost has no obvious acidity and Al-containing MCM-41 material prepared by partial replacement of Si ions with Al ions can improve the acidity of MCM-41. Prior literature has concluded that phosphorus modification is an effective way to optimize the acidity of zeolite and thus improve catalytic performance [9, 10]. Therefore, a series of phosphorus modified Al-MCM-41 zeolites were synthesized. Their performance on the activity, selectivity and stability in the selective transformation of ethyl mercaptan was evaluated. To the best of our knowledge, no detailed studies have been reported on this topic.

2 Experimental

2.1 Catalyst preparation

Al-MCM-41 (Si/Al = 20) zeolite was purchased from Catalyst Plant of Nankai University (Tianjin, China) and used as parent sample. Phosphorus modified samples were prepared by impregnating Al-MCM-41 with an aqueous solution containing the desired amount of P. The slurry was mixed thoroughly and placed in open air at room temperature for 24 h, followed by drying at 383 K for 3 h and calcining at 773 K for 4 h. The P loadings in the P modified samples were 2, 4, and 6 wt%, respectively. The prepared samples were denoted as PA-x, where x represented the phosphorus content.

2.2 Catalyst characterization

The chemical composition of the samples was measured by ICP-OES (Vista MPX, Varian Company). N_2 adsorption was conducted on the Quantachrome Autosorb-1 Instruments. The catalysts were outgassed at 573 K for 6 h and then measured by N_2 adsorption–desorption at 77 K. The powder X-ray diffraction (XRD) patterns of the catalysts were recorded on a PANalytical X'Pert Pro diffractometer using Cu Ka ($\lambda = 1.54056$ Å) radiation source operated at 45 kV and 30 mA. Data were collected in the range of $2\theta = 1°$–$10°$ with a step size of 0.02°.

Temperature-programmed desorption of ammonia (NH_3-TPD) was carried out on a conventional apparatus equipped with a thermal conductivity detector. The sample (0.1 g, 20–30 mesh) charged in a quartz tube was pretreated in a N_2 flow of 50 mL/min at 773 K for 2 h, and then cooled to ambient temperature. NH_3 was supplied to the sample as pulses through a six-way valve until saturation adsorption and a flat baseline was obtained. After flushing with nitrogen at 373 K for 1 h to remove physically adsorbed NH_3, the TPD profile was obtained by heating the sample from 373 to 823 K at a rate of 15 K/min. The desorbed NH_3 was trapped in boric acid followed by titration with a standard H_2SO_4 solution.

Solid state magic angle spinning nuclear magnetic resonance spectrometry (MAS-NMR) was carried out to characterize the Al and P environment in the samples. ^{27}Al and ^{31}P NMR spectra were obtained by a Varian Infinity-Plus 300 NMR spectrometer equipped with a MAS probe. ^{27}Al NMR spectra were working at 78.13 MHz with a spinning rate of 8.0 kHz, a pulse length of 0.6 μs and a pulse delay of 3.0 s. ^{31}P NMR spectra were recorded at 121.38 MHz with a spinning rate of 8.0 kHz, a pulse width of 1.0 μs and a pulse delay of 35.0 s. Chemical shifts were given in ppm from $Al(NO_3)_3$ (0 ppm) and 85 % as the external standard references for Al and P, respectively.

2.3 Catalytic performance evaluation

The decomposition of ethyl mercaptan was carried out in a fixed-bed reactor (stainless steel tube, i.d. = 9 mm) operated at atmospheric pressure. Prior to each experiment, 0.5 g of the catalyst (20–30 mesh) loaded in the constant-temperature zone was pretreated at 873 K for 2 h. After cooling to reaction temperature, ethyl mercaptan was fed into the reactor with weight hourly space velocities (WHSV) = 0.5 h^{-1}. Nitrogen was used as the carrier gas in this experiment. The feed composition was adjusted with flow meters to obtain the following gas mixtures: C_2H_5SH/N_2 (0.5/99.5, v/v). Standard experiments were performed at T = 693 K, P = 1 atm and WHSV of 0.5 h^{-1}. The products were analyzed online by gas chromatography equipped with a flame ionization detector and a flame photometric detector. At end of each experiment, the reactor was purged with nitrogen at the reaction temperature for 2 h to remove any possible residual reactants. The spent catalyst was unloaded and characterized by thermogravimetric analysis (TG) on a Perkin-Elmer Pyris 6 analyzer in air flow-rate of 100 mL/min and a heating rate of 10 K/min from room temperature to 1073 K.

3 Results and discussion

3.1 Physicochemical properties

The low-angle powder XRD patterns of the zeolites are displayed in Fig. 1. All sample exhibit a typical peak around 2.3° and a broad peak around 5°, indicating that the catalysts maintained the hexagonal structure and no additional phases emerged [11]. However, the phosphorus modified samples presented a clear decrease in intensity

around 2.3°. This can be attributed to the partial loss of long-range structural ordering, which may be caused by the formation of $AlPO_4$ species [12, 13]. As shown in Fig. 1, the peak positions of different samples around 2.3° showed a tendency toward the wide angle with the introduction of different phosphorus contents. This implies the framework collapse of the P-modified samples [14].

Table 1 lists the chemical composition and physical properties of the parent and phosphorus modified samples. As shown in Table 1, the specific surface area and pore volume decreased significantly with phosphorus addition. For example, when PA-0 was transferred to PA-4, the specific surface area and pore volume reduced from 978 m^2/g and 0.915 cm^3/g to 816 m^2/g and 0.740 cm^3/g, respectively. After loading with 6 % H_3PO_4, the specific surface area and pore volume further reduced to 528 m^2/g and 0.490 cm^3/g. This may be due to the formation of new $AlPO_4$ species outside or near pore entrances, which partially blocked zeolite channel openings [15–17].

Figure 2 shows the NH_3-TPD profiles of the parent and phosphorus modified Al-MCM-41 catalysts. Acid concentrations with differing strengths are summarized in Table 1. All samples produced two desorption peaks around 410 and 580 K, which represented ammonia desorption from weak and intermediate acid sites [18–20]. After modification with phosphorus, the high-temperature peak gradually shifted to a lower temperature and lost its intensity, suggesting that the strength and concentration of intermediate acid sites decreased. This can be ascribed to the removal of aluminum from the zeolite framework caused by phosphorus modification and subsequent calcinations [21]. With increased phosphorus content, the weak acid peaks also shifted toward lower temperatures, but the number of weak acid sites first increased and then decreased (Table 1). These observations imply that the appropriate amount of phosphorus addition can generate some new weak acid sites, but higher phosphorus contents lead to a decrease in weak acid sites [22].

The coordination state has noticeable impact on the acidity of zeolites. In order to investigate the influence of different trivalent framework atoms on the acidic properties, ^{27}Al and ^{31}P NMR of the catalysts are performed. As shown in Fig. 3a, there are two peaks in the ^{27}Al NMR

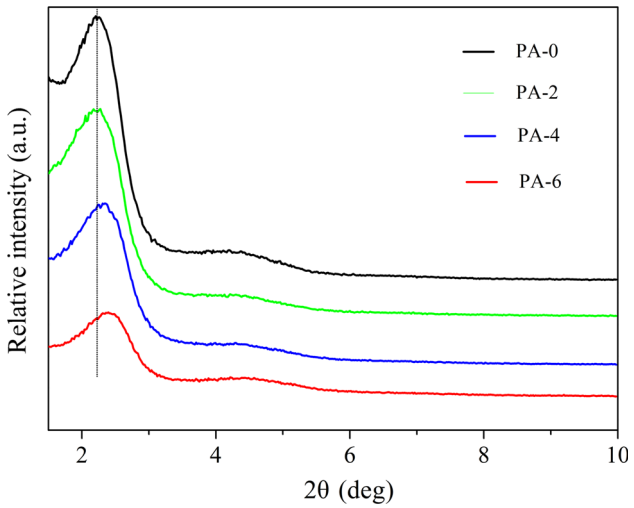

Fig. 1 XRD patterns of the catalysts

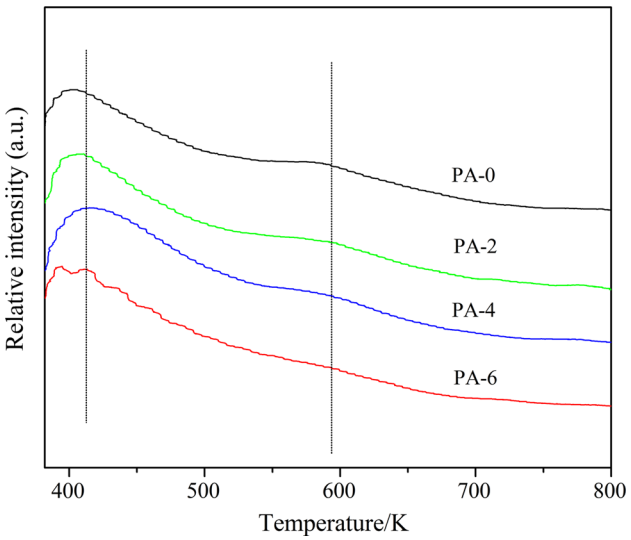

Fig. 2 NH_3-TPD profiles of parent and P-modified samples

Table 1 Physical and acidic properties of the catalysts

Samples	Al/P[a]	S_{BET} (m^2/g)	Pore volume (cm^3/g)	Pore diameter (Å)	Weak acid sites (mmol/g)	Intermediate acid sites (mmol/g)
PA-0	–	978	0.915	37.4	0.614	0.301
PA-2	3.57	853	0.777	36.4	0.705	0.261
PA-4	2.95	816	0.740	37.1	0.964	0.246
PA-6	1.27	528	0.490	36.1	0.698	0.214

[a] Real molar ratio of Al/P in the sample

spectra of PA-0, which can be assigned to tetrahedral Al in the zeolite framework (53 ppm) and octahedral Al in the extra-framework (0 ppm), respectively. Upon P modification, three peaks are observed in PA-4 at 53, 42 and −14 ppm. The new signal appeared at 42 ppm can be attributed to aluminum–phosphorus species formed by the interaction between P and framework Al. This provides evidence of the existence of P–O–Al structure that tetrahedral Al bonded to phosphorus atoms via oxygen bridges [23]. Additionally, chemical shift at −14 ppm was assigned to octahedral Al attached to phosphorous (aluminium phosphates).

^{31}P MAS NMR spectrum of PA-4 shows a broad peak at −23 ppm. Previous studies linked this signal to new P species which was formed through the reaction between phosphate and silanol left by dealumination. Consequently, partial Al–O bond in the Al–O–Si should be broken and the new P species (P–O–Si) was formed through the interaction between P and Al–O. From the above analysis, the formation of Si–O–P–O–Al structure seems to be favored than Si–O–Al–O–P bridges at the surface of MCM-41 [24]. This is in line with the results of TPD, the amount of surface acidic OH groups increased with the formation of Si–O–P–O–Al. The amount of bridge bonded hydroxyl group decreases due to the replacement of bridge bonded hydroxyl group by ($H_2PO_4^-$). Thus, the desorption area of weak acid sites increases while the intermediate acid sites decreases [25, 26].

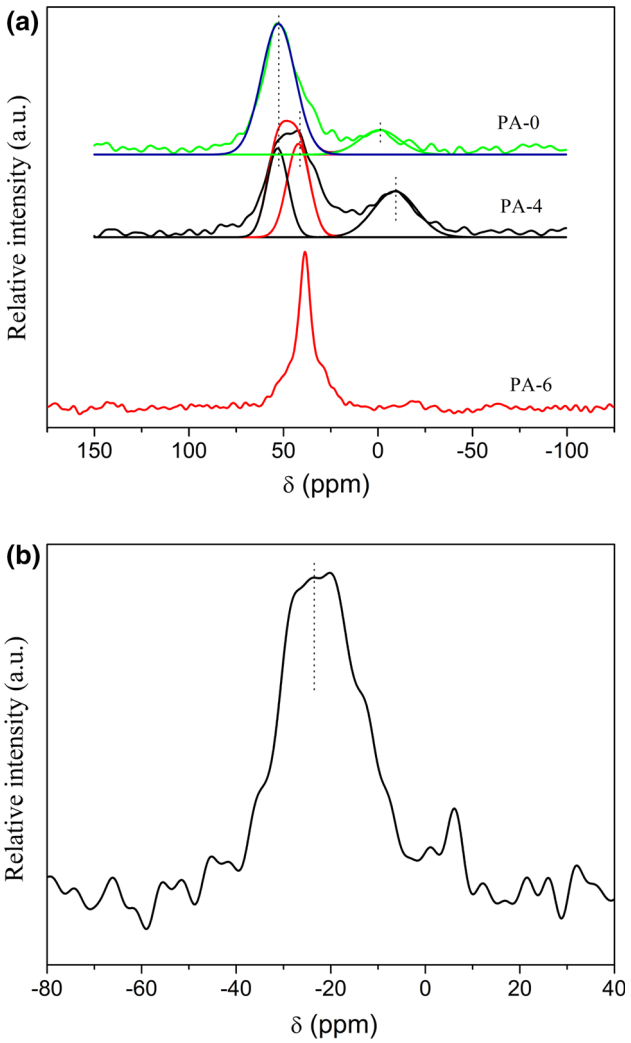

Fig. 3 MAS NMR spectra of the catalysts **a** ^{27}Al and **b** ^{31}P

3.2 Catalytic conversion of ethyl mercaptan

As a blank experiment without any catalyst, ethyl mercaptan conversion remained below 5 % all the time at 693 K. While at the same temperature, the conversions of ethyl mercaptan were all higher than 95 % over the parent and modified Al-MCM-41 samples, indicating that this reaction was a catalysis process. Catalytic testing of the conversion of ethyl mercaptan was carried out at WHSV = 0.5 h^{-1}, reaction temperature = 693 K.

The catalytic performances of different catalysts are investigated and the conversion and stability results are presented in Fig. 4. To obtain a quantitative measurement of stability, the lifetime of the catalysts is defined as the time at which the initial conversion (TOS = 1 h) drops by 5 %. Initially (TOS = 1 h), the conversion of all the P modified samples are above 99 %, a little higher than 97.8 % of PA-0, indicating that the presence of P has positive effect on the conversion of ethyl mercaptan. As shown in Fig. 1, the lifetime of PA-0 is only 19 h, while the conversion of PA-2 drops by 5 % within 31 h. With the increase of P content, the lifetime of PA-4 extends to 77 h. However, when further increased P content on PA-6 brings about negative effect and deactivation is observed after

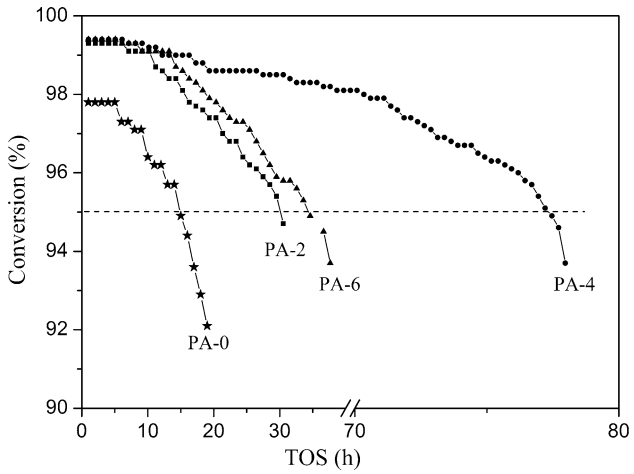

Fig. 4 Conversion of ethyl mercaptan with TOS of the catalysts. Reaction: T = 693 K, P = 1 atm, WHSV = 0.5 h^{-1}

Table 2 Products distribution on catalysts at 693 K and 10 h tos

Sample	Selectivity to S products		Selectivity to C products		Coke (mg/100 mg)
	H_2S	Others[a]	C_2H_4	Others[b]	
PA-0	87.4	12.6	85.7	14.3	3.1
PA-2	94.5	5.5	92.1	7.9	2.0
PA-4	97.1	2.9	96.4	3.6	0.9
PA-6	95.6	4.4	93.8	6.2	1.1

[a] Mainly CS_2

[b] Mainly C1–C4 alkanes and BTX

37 h. This shows that the decomposition of ethyl mercaptan strongly depends on the amount and strength of the weak acid sites. Desorption of ethylene is fast due to its relative weak acidity and thus by-reactions are prevented. From the NH_3-TPD results, it can be found that the incorporation of P increases the concentration of weak acid sites notably. Therefore, the better stability of PA-4 than PA-2 and PA-6 may be ascribed to more weak acid sites, and higher concentration of weak acid sites is beneficial for the stability of the catalysts.

Table 2 displays product distributions of the ethyl mercaptan decomposition on different catalysts. For all tests, the carbon balance was very accurate. The catalytic test was carried out using the fresh sample for 10 h time-on-stream. The formation of ethylene and hydrogen sulfide largely prevails in this experiment. And the main by-products are diethyl sulfide, CS_2, as well as benzene, toluene and xylene (BTX). The selectivity presented in Table 2 are values averaged over the 10 h tos. The traces amount of thiophene reported before is not present in our research. The selectivity for ethylene over P modified zeolites is higher than that of PA-0. However, the loading up to 6 % H_3PO_4 leads to a decrease in selectivity to 93.8 %. This indicates that the selectivity for ethylene strongly depends on the amount and strength of the acid sites. Our results indicate that more abound weak acid sites combined with certain acid strength are favorable to the formation of ethylene. Therefore, 4 % loadings is optimum P content for obtaining high ethylene selectivity in our present investigation.

The investigation of deactivation behavior has a certain guiding significance for the improvement of catalytic performance. TG–DTA analysis was performed to try to figure out the relations of the deposited carbon and stability at different reaction temperatures. The coke content was measured at tos = 10 h. Among the four samples, PA-0 shows the largest amount of coke (3.1 g). P modification can reduce the coke formation significantly and the coke that preferentially formed on intermediate acid sites is considerably inhibited. Additionally, the hard coke was preferentially formed on the intermediate acid sites and P modification decreased its strength and concentration remarkably, thus improves the catalyst's anti-coking ability and prolong lifetime. To gain a better insight into the catalyst deactivation, long-term experiments (72 h) were carried out at 693 K in the presence of PA-4 sample. The coke amount at TOS = 72 h is only slightly higher than that built up after 10 h of reaction, pointing out that the coke is generated mainly at the early stage of the process.

4 Conclusions

In present work, we explore the catalytic performance of parent and P modified Al-MCM-41 zeolites for the decomposition of ethyl mercaptan. Introduction of phosphorus in Al-MCM-41 leads to a decrease of intermediate acid strength and concentration, along with the formation of new weak acid sites. And variation of P loadings enables modifying of the acidity. The catalytic performance results reveal that P modification can effectively improve the ethylene selectivity and prolong catalyst lifetime. The highest activity and selectivity were observed on PA-4 with the appropriate weak acid sites and acid strength. The selective catalytic conversion of mercaptans (ethyl mercaptan) into H_2S and hydrocarbons over acid solid catalysts could be incorporated as a stage into an integrated system, including the adsorption/desorption of sulfur compounds on molecular sieves.

References

1. C. Cammarano, E. Huguet, R. Cadours, B. Coq, V. Hulea, Appl. Catal. B **156**, 128–133 (2014)
2. V. Hulea, E. Huguet, C. Cammarano, A. Lacarriere, R. Durand, C. Leroi, R. Cadours, B. Coq, Appl. Catal. B **144**, 547–553 (2014)
3. D. Gao, A. Duan, X. Zhang, Z. Zhao, E. Hong, Y. Qin, C. Xu, Chem. Eng. J. **270**, 176–186 (2015)
4. D. Gao, A. Zheng, X. Zhang, H. Sun, X. Dai, Y. Yang, H. Wang, Y. Qin, S. Xu, A. Duan, Nanoscale **7**, 10918–10924 (2015)
5. A. Samuels, I. Fox, U.S. Patent 5478541, 1995
6. E. Gal, U.S. Patent 20080267847, 2008
7. A. Ryzhikov, V. Hulea, D. Tichit, C. Leroi, D. Anglerot, B. Coq, P. Trens, Appl. Catal. A **397**, 218–224 (2011)

8. D. Zhang, R. Wang, X. Yang, Catal. Commun. **12**, 399–402 (2011)
9. E.G. Vaschetto, G.A. Monti, E.R. Herrero, G.C. Sandra, A.E. Griselda, Appl. Catal. A **453**, 391–402 (2013)
10. Q. Qiao, R. Wang, M. Gou, X. Yang, Microporous Mesoporous Mater. **195**, 250–257 (2014)
11. M. Li, H. Wang, X.Q. Li, J.R. Liu, Adv. Mater. **779**, 201–204 (2013)
12. S. Ajaikumar, A. Pandurangan, J. Mol. Catal. A-Chem. **266**, 1–10 (2007)
13. M. Stekrova, P. Zizkova, E. Vyskocilova, J. Kolena, L. Cerveny, J. Porous Mater. **22**, 73–81 (2014)
14. T.D. Conesa, R. Mokaya, J.M. Campelo, A.A. Romero, Chem. Commun. **17**, 1839–1841 (2006)
15. F. Thibault-Starzyk, A. Vimont, J.-P. Gilson, Catal. Today **70**, 227–241 (2001)
16. K. Damodaran, J.W. Wiench, S.M. Cabral de Menezes, Y.L. Lam, J. Trebosc, J.-P. Amoureux, M. Pruski, Microporous Mesoporous Mater. **95**, 296–305 (2006)
17. J.A. Lercher, G. Rumplmayr, Appl. Catal. **25**, 215–222 (1986)
18. S. Kawi, S.C. Shen, P.L. Chew, J. Mater. Chem. **12**, 1582–1586 (2002)
19. G. Caeiro, P. Magnoux, J.M. Lopes, F. Ramôa Ribeiro, S.M.C. Menezes, A.F. Costa, H.S. Cerqueira, Appl. Catal. A **314**, 160–171 (2006)
20. Z.Y. Yuan, T.H. Chen, J.Z. Wang, H.X. Li, Colloids Surf. A Physicochem. Eng. Aspects **179**, 253–259 (2001)
21. H. Kosslick, G. Lischke, B. Parlitz, W. Storek, R. Fricke, Appl. Catal. A **184**, 49–60 (1999)
22. N.H. Xue, X.K. Chen, L. Nie, X.F. Guo, W.P. Ding, Y. Chen, M. Gu, Z.K. Xie, J. Catal. **248**, 20–28 (2007)
23. K. Góra-Marek, J. Datka, Appl. Catal. A **302**, 104–109 (2006)
24. M. Ghiaci, H. Aghaei, M. Oroojeni, B. Aghabarari, V. Rives, M.A. Vicente, I. Sobrados, J. Sanz, Catal. Commun. **10**, 1486–1492 (2009)
25. K.Y. Kwak, M.S. Kim, D.W. Lee, Fuel **137**, 230–236 (2014)
26. D. Qi, A. Duan, Z. Zhao, J. Porous Mater. **22**, 127–135 (2015)